Half-metallic Ferromagnetism in Non-magnetic Double Perovskite Oxides Sr_2MSbO_6 (M=Al, Ga) Doped with C and N.

AMRANI Bouhalouane (abouhalouane@yahoo.fr)
Universite d'Oran 1 Ahmed Ben Bella
Djilali BENDJEBBOUR
Universite d'Oran 1 Ahmed Ben Bella
Tayeb SEDDIK
Universite Mustapha Stambouli Mascara
Mohamed Walid MOHAMED
Centre Universitaire Ain Temouchent
driss khdoja
Universite d'Oran 1 Ahmed Ben Bella

Research Article

Keywords: Double perovskite oxides, First-principles calculations, half metallicity, non-magnetic 2p-impurities.

Posted Date: December 30th, 2021

DOI: https://doi.org/10.21203/rs.3.rs-1160298/v1

Abstract

Double perovskite oxides have gained tremendous attention in material science and device technology due to their facile synthesis and exceptional physical properties. In this paper, we elucidate the origin of magnetization in non magnetic double perovskite oxides Sr_2MSbO_6 (M=Al, Ga) induced by non-magnetic 2*p*-impurities (C and N) substituted. The calculations were done within the full potential linearized augmented plane wave method (FP-LAPW) in the framework of the density functional theory (DFT). The exchange-correlation potential is evaluated using the generalized gradient approximation (GGA) of Perdew–Burke–Ernzerhof (PBE) and the modified Becke and Johnson (mBJ-GGA). Regarding structural properties of undoped double perovskites Sr_2MSbO_6 (M=Al, Ga), we found that the lattice constants and oxygen positions are in rational accord with the experimental results. Furthermore, both of the examined compounds are brittle in nature with isotropic character. For Sr_2AlSbO_6 we have got the values of energy gap equal to 1.9 eV and 3.7 eV within the GGA and the mBJ-GGA, respectively. However for Sr_2GaSbO_6 the values of energy gap obtained in GGA and mBJ-GGA are equal to 0.8 eV and 2.9 eV, respectively. Finally, spin-polarized calculations reveal that the doping C and N can lead to drastic changes in the magneto-electronic properties of the semiconducting Sr_2MSbO_6 matrix with the integer magnetic moment of 6.00 μ_B and exhibit half-metallic properties. The origin of ferromagnetism can be attributed to the spin–split impurity bands inside the energy gap of the semiconducting Sr_2MSbO_6 matrix. These results may help experimentalists in synthesizing new double perovskites for spintronic applications.

1. Introduction

The field of spintronics, also known as spin electronics, can be referred to as one of the most important and promising branches of materials science and condensed matter [1–3]. For spintronic applications, materials must have high spin polarization, high magnetic moment, and high Curie temperature. Some half-metallic ferromagnetic materials which can be considered as hybrids between semiconductors and metals are used in spintronic applications such as spin valves [4–7], spin filters [8], magnetic sensors [9, 10], memory storages [11–13], and tunneling magnetoresistance effect [14–17]. Most representative half-metallic materials belong to either Heusler alloys (full, half, as well as quaternary) [18–25] or dilute magnetic semiconductors [26–30] or transition metal oxides in different chemical compositions and structural types, such as perovskites [31–34] or double perovskites [35–47]. Another widely discussed scenario for d^0 dilute magnetic semiconductors is based on a quite unexpected effect of magnetization of non-magnetic matrix induced by nonmagnetic *2p* impurities [31].

Strontium-based double perovskites have always been one of the most important members of half-metallic magnetic materials due to their robust half-metallicity and high Curie temperature. The search of new double perovskite in term of their composition, structure and functionality to get desired properties is an active area of research in material science and beyond. Many different properties have been explored in these strontium double perovskites, such as half-metallic behavior in Sr_2FeMO_6 (M =Mo, Re) and Sr_2CrMO_6 (M=Mo, W) [36–39], tunnel magnetoresistance in Sr_2FeMoO_6 [40], room-temperature colossal

magnetoresistance in Sr_2MMoO_6 (M = Cr, Fe) [37, 39], magnetoelectric in Sr_2CoMoO_6 [41], and half-metallic antiferromagnetic in Sr_2OsMoO_6 [42]. To the best of our knowledge, only a few studies on Sr_2(Ga, Al)SbO_6 have been reported until now [48–51]. Experimentally, both compounds have a cubic structure at room temperature with space group Fm3m. Sr_2AlSbO_6 has been prepared, and characterized by X-ray diffraction (XRD) in [48], and it was reported that this compound adopt the cubic phase with the lattice parameter a = 7.766 A-7.763 A. In the same context, Wittmann et *al.* [49] reported the synthesis and phase transitions of Sr_2GaSbO_6 using powder neutron diffraction “X-ray diffraction analysis” and confirm the cubic structure with a lattice constant of 7.89 Å. As the reported experimental results are limited just to the structure, the elastic, mechanical and electronic properties are still undiscovered; therefore, these materials need further investigation to understand their properties and increase their applications. The present work provides us understanding of the magnetization induced in semiconducting Sr_2MSbO_6 (M = Al, Ga) matrix and a deep comprehension of the relationship between their magnetic and electronic properties. Furthermore, our contribution covers the deficiency on the fundamental properties of these Sr-based double perovskite oxides Sr_2MSbO_6.

2. Computational Details

The calculations of undoped and doped Sr_2MSbO_6 (M=Al, Ga) double perovskites were carried out by using the full-potential linearized augmented plane-wave method implemented in the WIEN2K code [52, 53] within the scheme of density functional theory [54]. For the exchange–correlation effects, we have used the generalized gradient approximation (GGA) [55]. Moreover, the modified Beck Johnson *(*mBJ*)* potential was applied to overcome the inefficiency of the GGA functional to predict the magneto-electronic properties [56].

The charge density of Fourier expansion and maximum values of angular momentum were set to be l_{max} = 10, and G_{max} = 14 respectively. To certify that there is no outflow of charge from core, non-overlapped muffin-tin radius (R_{MT}) and converged energy value should be selected. The kinetic energy cut-off of R_{MT}* K_{max} is equal to 8. The convergence criteria used for energy was 10^{-4} Ry, whereas the charge was converged up to 10^{-3}e. A dense k-mesh of 20 × 20 ×20 was used to calculate all physical properties of considered compounds, and the separation between the core and valence states was set to -6.0 Ry.

3. Results And Discussion

The results obtained using the various ground state parameters are discussed as below

3.1. Fundamental properties of undoped double perovskites Sr_2MSbO_6 (M=Al, Ga)

3.1.1. Structural properties and stability of Sr_2MSbO_6 (M=Al, Ga)

The stability of non magnetic double perobvskites Sr_2MSbO_6(M=Al, Ga) strongly depends on the ionic radii of the constituting metal ions, which is generally assured by the Goldschmidt tolerance (t) factor [57]. For Sr_2MNbO_6 (M= Al, Ga), t can be calculated via the:

$$t = \frac{\left(r_{Sr} + r_O\right)}{\sqrt{2}\left(r_{M,Sb} + r_O\right)} = \frac{\sqrt{2}\left(r_{Sr} + r_O\right)}{\left((r_M + r_{Sb}) + 2r_O\right)}$$

1

where r_{Sr}, r_O, r_{Sb}, r_M are the ionic radii of Sr, O, Sb and M(M=Al, Ga) respectively [58]. For an ideal cubic phase, the value of the tolerance factor t is equal to or near unity. It may be seen from the Table1 that the calculated tolerance factor t for $Sr_2^{2+}Al^{3+}Sb^{5+}O_6^{2-}$ is 1.011 and for $Sr_2^{2+}Ga^{3+}Sb^{5+}O_6^{2-}$ is 0.991, confirming the stability of the cubic phase.

Table 1

The calculated and experimental crystallographic data for Sr_2MSbO_6 (M = Al, Ga); tolerance factors (t), Glazer tilt system (GTS), lattice constants a, oxygen positions u, bulk modulus (B), pressure derivative of bulk modulus (B'), standard enthalpy of formation energies (ΔH_f^O), and the average bond-lengths. Values within parentheses represent the predicted results at RT via the SPuDS Software.

	Sr_2AlSbO_6		Sr_2GaSbO_6	
	Our work	**Exp**	**Our work**	**Exp**
t	1.011	1.021[48]	0.991	0.999[49]
GTS	$a^0a^0a^0$		$a^0a^0a^0$	
a (Å)	7.859(7.780)	7.766 [48]	7.979 (7.938)	7.890[49] 7.891[50]
u	0.254 (0.245)	0.252[48]	0.250 (0.250)	0.239[50]
B (GPa)	158.426		149.802	
B’	4.581		4.614	
ΔH_f^O(kJ/mol)	-256.747		-239.284	
M(4a)-O(24e) · 6 (Å)	1.9336(1.9075)		1.9950 (1.9865)	1.888[50]
Sr(8c)-O(24e) · 12(Å)	2.7791 (2.7508)		2.8214(2.8064)	
Sb(4b)-O(24e) · 6 (Å)	1.9964 (1.9824)		1.9950(1.9824)	2.057[50]

Table.2. Calculated elastic constants C_{ij}, shear modulus G, young’s modulus E, poisson’s ratio *v*, Anisotropy factor A and B/G ratio of Sr_2(Al ,Ga)SbO_6. The units for Cij, G, E are GPa

	Sr_2AlSbO_6	Sr_2GaSbO_6
C11	296.600	284.036
C12	88.879	82.684
C44	102.198	99.276
G	102.857	99.829
E	253.585	245.053
υ	0.233	0.227
A	0.984	0.986
B/G	1.537	1.501

The crystal structure of the cubic Sr_2MSbO_6(M=Al, Ga) is shown in Figure 1. The Wyckoff positions of Sr, M, Sb, O are located at 8c(1/4, 1/4, 1/4), 4a(0, 0, 0), 4b(1/2,0,0), 24e(0.254,0,0), respectively. The bond angle <M–O–Sb> = 180° and thus no MO_6–SbO_6-octahedral distortions. The tilting of the octahedra is the primary source of deviation from the cubic structure and can be described by using the Glazer tilt system (GTS) [59, 60]. Therefore, no octahedra tilting or ($a^0a^0a^0$) in the GTS notation exists in Sr_2MSbO_6, as illustrated in Table 1. The overall structure stability can be evaluated by the global instability index (GII), i.e. the deviation of the bond valence sums with the ideal formal valences [61, 62]. The GII value is usually lower than 0.1 v.u., valence units, for unstrained structures and as large as 0.2 v.u. in a structure with lattice-induced strains [62]. The GIIs of Sr_2MSbO_6 (M= Al, Ga) are determined using the Structure Prediction Diagnostic Software [63] and gives the values of 0.0876 v.u. and 0.0686 v.u., respectively.

Next, to obtain the structural properties of Sr2MSbO6, we perform the optimization by calculating the total energies for different volumes and by fitting the values to the Murnaghan's equation of state [64]. The optimized parameters are summarized in Table 1 and obtained values are in rational accord with the experimental measurements [48–51]. In regard to the oxygen position u, the results found to be around the ideal value 0.25. Additionally, the structural parameters were also predicted using the ionic crystal model [63]. Hence, it was concluded that the optimized parameters are consistent with the predicted values. We can note also that the bulk modulus decreases as the lattice parameter increases when traversing from Al to Ga in Sr2MSbO6.

In practical applications, the thermodynamic stability of new materials is an important parameter that affects their selection and use. In order to confirm the thermodynamic stability of double perovskite oxides Sr2MSbO6, the enthalpy of the formation energy ΔH_f^o was examined by calculating the energy difference ΔE between the double perovskite Sr_2MSbO_6 and existing materials, such as M_2O_3 (M=Al, Ga) and SbO_3 based on their thermochemical equations using the solid state reaction procedure as follows:

$4SrCO_3 + M_2O_5 + 2SbO_2 + H_2 \rightarrow 2Sr_2MSbO_6 + 4CO_2 + H_2O$ (2)

Hence, ΔH_f^o can be expressed in the following equation:

$$\Delta H_f^o = \Delta E = E_{Tot} - \sum_i^N n_i E_i = 2E_{Tot} - (n_1 E_{Sr} + n_2 E_M + n_3 E_{Sb} + n_4 E_{O_2})$$

3

Where E_{Tot} is the total energy per unit cell volume (Z = 2) of Sr_2MSbO_6, $E_i = E_{Sr}$, E_M (M = Al and Ga), E_{Sb} and E_O are the energy of individual elements in the unit cell, and ni denotes the number of atoms of the ith element in a single formula unit; $n_1 = 4$, $n_2 = 2$, $n_3 = 2$, and $n_4 = 6$, respectively. The calculated formation energies are negative for both double perovskites Sr_2MSbO_6, which indicates that those compounds are in the thermodynamic stability.

This result is not surprising when we know that Sr_2MSbO_6 have been already experimentally synthesized. On the other hand, it is important to observe that the average bond distances in Sr_2AlSbO_6 are very similar to those in Sr_2GaSbO_6. This is can be attributed to the fact that the ionic radii of Al^{3+} and Ga^{3+} are nearly equal.

3.1.2. Elastic properties and mechanical stability of Sr_2MSbO_6 (M=Al, Ga)

Generally, there is a mere fact of having structural stability does not guarantee the existence of the double perovskite structure. However, to some extent, the stability can be characterized qualitatively by the mechanical stability criteria. To predict the independent elastic constants, one can use the volume conserving tetrahedral and rhombohedral distortions on the cubic phase of Sr_2MSbO_6. The obtained values of the elastic constants are listed in Table 2. To our best knowledge, no studies have been conducted concerning the elastic constants. Therefore, our results can be assumed to be predictive. Obviously, the elastic constants of these two double perovskites Sr_2MNbO_6 satisfy the mechanical stability criteria [65]. Subsequently, using the elastic constants to predict the polycrystalline moduli, the shear modulus (G), young modulus (E), poisson's ratio (υ) and shear anisotropic factor (A) (also called Zener coefficient). The calculated data are also listed in Table 2. To classify the materials in ductile manner or brittle manner we use the relationship proposed by Pugh [66, 67] which links empirically the plastic properties of metals with their elastic moduli by B/G known as Pugh's ratio. A material with B/G smaller than 1.75 and υ smaller than 0.26 is brittle, otherwise it is ductile. From Table 2, it shows that values of B/G and ν are smaller than 1.75 and 0.26 respectively, confirming that Sr_2MSbO_6 double perovskites are brittle.

Young's modulus (E) is defined as the ratio of stress and strain when Hooke's law holds. The Young's modulus of a material is the usual property used to characterize stiffness. As the Young's modulus increases, the stiffness of compound increases too. Thus, the Sr_2AlSbO_6 is stiffer than Sr_2GaSbO_6, as revealed in Table 2. Another important mechanical quantity is the elastic anisotropy factor A, which gives a measure of the anisotropy of the elastic wave velocity in a material. For an isotropic material, A is equal to unity, while any value smaller or larger than unity indicates anisotropy. From the computed anisotropy values that are listed in Table 2, one can conclude that these two values confirm the elastically isotropic-like character. To date, no experimental or theoretical data for these properties are available in the literature to be compared with our theoretical results therefore, future experimental work may testify our calculated predictions.

3.1.3. Electronic properties of Sr_2MSbO_6 (M=Al, Ga)

In order to investigate the electronic properties of undoped Sr_2MSbO_6, we focus our study on the electronic band structure and the density of states (DOS). As shown in Figure 2, the calculated band structures along the higher symmetry directions in the irreducible Brillouin zone (IBZ) were evaluated with both PBE-GGA and mBJ-GGA approximations. The zero of energy corresponds to the Fermi level. The

occupied states below the Fermi energy correspond to the valence band, whereas the unoccupied states lying above the Fermi energy correspond to the conduction band. The overall band profiles are found to be the same for both double perovskites and show that these materials have a direct energy band gap at center of Brillouin zone Γ. For Sr_2AlSbO_6 we have got the values of energy gap equal to 1.9 eV and 3.7 eV within the GGA and the mBJ-GGA, respectively. However for Sr_2GaSbO_6 the values of energy gap obtained in GGA and mBJ-GGA are equal to 0.8 eV and 2.9 eV, respectively. Unfortunately, there are no reported experimental measurements or previous theoretical calculations of the band gaps for the considered compounds to be compared to the present results. It is important to mention that, mBJ-GGA gives the more accurate band gap energy of the semiconductors and insulators, whereas the GGA functional fails qualitatively [31, 68–70]. To aid in understanding the character of electronic structures, we have calculated the total densities of states (TDOS) and partial densities of states (PDOS) for these double perovskites Sr_2MSbO_6 by using mBJ-GGA and the corresponding results are shown in Figure 3. Our calculations suggested that the lower part of the valence band is dominated

by the Sb 5*s* orbital, and the upper part by the O 2*p* orbital in Sr_2MSbO_6. The lower part of the conduction band is dominated by the Sb 5*s* orbital.

3.2 Magnetization of $Sr_2(Al,Ga)SbO_6$ induced by C and N impurities

As mentioned before, double perovskite oxides offer an important number of interesting physicochemical properties and high potential for technological applications, many of which are still not fully understood, and can be substantially modified through doping impurities. In particular, the light elements (C and N) mono-doping as anions to replace oxygen have attracted much attention and are considered one of the appropriate anions alloys elements because its sizes are closer to the size of the substituted host oxygen atoms, which are favorable for effective incorporation. In this section, we tried to study the magnetism induced by the 2*p*-impurities in non-magnetic double perovskite oxides Sr_2MSbO_6 (M=Al, Ga) for possible applications in spintronic and magneto-electronic devices. The results were obtained in calculations using the 2×1×1 supercell (in the x, y and z directions) containing 40 atoms. From this 40-atoms supercell, oxygen was substituted with an impurity atom X (X= C or N). Our corresponding systems have been written under the formula composition $Sr_2MSbO_{5.75}X_{0.25}$ where M=Al, Ga and X= C and N. After creating a supercell with one centrally placed impurity atom X, *a* complete relaxation was done. In order to check the stability of ferromagnetic state, we calculated the spin polarization energy (ΔE_{sp}), which is the energy difference between the spin-polarized and non-spin polarized states of these doped systems. We found that the ferromagnetic state is more stable than nonmagnetic state.

To explore the mechanism of induced ferromagnetism, the densities of states for doped (C and N) double perovskites have been computed using both GGA and mBJ exchange-correlation functional. The results obtained for the densities of sates of these compounds are nearly same, in both GGA and mBJ schemes. Figure.4 exhibits densities of states obtained using mBJ functional for C and N doped Sr_2MSbO_6. It is

evident from this figure that when 2p impurities are incorporated, these compounds are true half-metallic in nature. In this case, we can attribute the origin of this magnetization to the presence of strong exchange splitting in the density of states of C and N impurities. The major contribution to the DOS at the Fermi level comes from the 2*p* states of impurities and by 2*p* states of oxygen atoms nearest to the impurity. Due to this, it is clear that the system exhibits hole induced 2p ferromagnetism. The magnetic moments predicted from our calculations are depicted in Table 3. The results confirms that C or N doped Sr_2MSbO_6 (M=Al, Ga) compounds are half-metallic ferromagnetic with a total magnetic moment of 6.00 μ_B under GGA and mBJ calculations. According to Hund's rule coupling, the total magnetic moment in the supercell is equal to the number of doped holes [31, 71].

Table 3. Calculation of the spinpolarized and total magnetic moments M_{tot} for cubic double perovskite oxides Sr_2MSbO_6 (*M* = Al and Ga) doped with 2*p* impurities (*X* = C and N) and the relative contribution (%) of the Sr atom moment (M_{Sr}), M atom moment (*M*=Al or Ga), Sb atom moment (M_{Sb}), O atom moment (M_O) and interstitial moment (M_{int}) in Bohr magnetons.

Compounds		M_{Sr}	M_M	M_{Sb}	M_O	M_X	M_{int}	M_{tot}
$Sr_2AlSbO_{5.75}C_{0.25}$	GGA	0.011	0.034	0.048	0.046	0.519	2.141	6.016
	mBJ-GGA	0.010	0.007	0.001	0.032	0.566	2.103	6.000
$Sr_2AlSbO_{5.75}N_{0.25}$	GGA	-0.057	-0.001	-0.015	0.057	0.628	1.490	5.999
	mBJ-GGA	-0.004	-0.001	-0.051	0.04685	0.797	0.788	6.000
$Sr_2GaSbO_{5.75}C_{0.25}$	GGA	0.012	0.030	0.042	0.052	0.483	2.179	6.009
	mBJ-GGA	0.1477	0.0024	0.023	0.009	0.556	2.449	6.000
$Sr_2GaSbO_{5.75}N_{0.25}$	GGA	0.00479	-0.001	-0.014	0.053	0.637	1.48649	6.001
	mBJ-GGA	-0.0035	-0.013	-0.049	0.038	0.810	0.807	6.000

4. Conclusion

In this paper, first-principles density functional theory calculations were performed in order to elucidate the origin of magnetization in non magnetic double perovskites Sr_2MSbO_6 (M=Al, Ga) doped with non-magnetic elements (C or N). Regarding structural properties of undoped double perovskites Sr_2MSbO_6 (M=Al, Ga), it has been found that the tolerance factor, formation energy, and stability criteria confirm the stability of these materials in the cubic phase. The lattice constants and oxygen positions are in rational accord with the experimental results. The analysis of mechanical parameters reveals that both

compounds are brittle in nature with isotropic behavior. More importantly, for Sr_2AlSbO_6 we have got the values of energy gap equal to 1.9 eV and 3.7 eV within the GGA and the mBJ-GGA, respectively. However for Sr_2GaSbO_6 the values of energy gap obtained in GGA and mBJ-GGA are equal to 0.8 eV and 2.9 eV, respectively.

Finally, spin-polarized calculations reveal that the doping C and N can lead to drastic changes in the magneto-electronic properties of the semiconducting Sr_2MSbO_6 matrix with the integer magnetic moment of 6.00 μ_B per cell and exhibit half-metallic properties. The origin of ferromagnetism can be attributed to the spin–split impurity bands inside the energy gap of the semiconducting Sr_2MSbO_6 matrix. The present theoretical estimation of various physical parameters can prove as valuable reference with respect to their future experimental work.

Declarations

Acknowledgement

This work was financially supported by the general directorate for scientific research and technological development under PRFU Project Number: B00L02UN310120190004.

References

[1] S. A. Mir, A.Q Seh, D. C. Gupta, RSC Adv.**10** (2020) 36241.

[2] S. D. Sarma, Am. Sci. **89** (2001) 516.

[3]V. K. Joshi, Eng. Sci. Technol. Int. J. **19** (2016) 1503.

[4] T. Kimura, Y. Otani, Phys. Rev. Lett. **99** (2007) 196604.

[5] X.J. Wang, H. Zou, L.E. Ocola, R. Divan, Y. Ji, J.Appl. Phys. **105** (2009) 093907.

[6] M. Erekhinsky, A. Sharoni, F. Casanova, I.K. Schuller, Appl. Phys. Lett. **96** (2010) 022513.

[7] A. Vogel, J. Wulfhorst, G. Meier, Appl. Phys. Lett. **94** (2009) 122510.

[8].P.Recher, E.V.Sukhorukov, D.Loss, Phys. Rev. Lett. **85** (2000) 1962.

[9] R. Bogue, Sens. Rev **34** (2014) 137.

[10] C.Reig, M.D.C.Beltrán, D.R. Muñoz, Sensors. **9** (2009) 7919.

[11] D.D. Sante, A.Stroppa, P.Jain, S.Picozzi, J. Am. Chem. Soc. **135** (2013) 18126.

[12] M. Alexe, M. Ziese, D. Hesse, P. Esquinazi, K. Yamauchi, T.Fukushima, S. Picozzi, U. Gösele, Adv. Mater. **21** *(*2009) 4452.

[13]. Q.Yang, W. Xiong, L. Zhu, G. Gao, M. Wu, J. Am. Chem. Soc. **139** *(*2017) 11506.

[14] D. Sánchez, Phys. Rev. B **79 (**2009) 045305.

[15]. H.Liu, Y.Honda, T.Taira, K.Matsuda, M.Arita, T. Uemura, M. Yamamoto, Appl. Phys. Lett. **101** (2012) 132418.

[16] F. Bonell , S. Andrieu , C. Tiusan , F. Montaigne , E. Snoeck , B. Belhadji, L. Camels , F. Bertran , P. Le Fèvre , A. T. Ibrahimi , Phys. Rev. B **82** *(*2010) 092405.

[17] T. Kubota , Y. Miura , D. Watanabe , S. Mizukami , F. Wu , H. Naganuma , X. Zhang , M. Oogane , M. Shirai , Y. Ando , T. Miyazaki , Appl. Phys. Express **4** (2011**)** 043002.

[18] S. Mizukami, D. Watanabe, M. Oogane, Y. Ando, Y. Miura, M. Shirai and T. Miyazaki, J. Appl. Phys. **105** (2009) 07D306.

[19] H. G. Zhang, C. Z. Zhang, W. Zhu, E. K. Liu, W. H. Wang, H. W. Zhang, J. L. Cheng, H. Z. Luo, G. H. Wu, J. Appl. Phys **114** (2013) 013903.

[20] H. Abbassa, S. Meskine, A. Labdelli, S. Kacher, T. Belaroussi, B. Amrani, Mat. Chem. Phys. **256** (2020) 123735.

[21] Y. Mouffok, B. Amrani, K. Driss Khodja, H.Abbassa, J. Super.Nov. Magn **32** (2019) 615.

[22] A. Abada, K. Amara, S. Hiadsi, B. Amrani, J. Magn.Magn. Mater. **388** (2015) 59

[23] H. Abbassa, S. H.Mebarki, B. Amrani, T. Belaroussi, K. Driss Khodja, J. Alloys .Compd **637** (2016) 557.

[24] M. Ram, A. Saxena, A. E. Aly, A. Shankar, RSC. Adv. **10** (2020) 7661.

[25] W. H. Wang, M. Przybylski, W. Kuch, L. I. Chelaru, J. Wang, Y. F. Lu, J. Kirschner, Phys. Rev. B **71** (2005) 144416.

[26] M. Venkatesan, C. B. Fitzgerald, J. G. Lunney, J. M. D. Coey, Phys. Rev. Lett **93** (2004) 177206.

[27] Z. Xu, Y. Li, Z. Liu, S.F. Liu, J. Magn. Magn. Mater. **451** (2018) 799.

[28] T. Fukumura, Z. Jin, A. Ohtomo, H. Koinuma, M. Kawasaki, Appl. Phys. Lett. **75** (1999) 3366.

[29] Z.Y. Feng, J.M. Zhang, J. Phys. Chem. Solids **114** (2018) 240.

[30] H.S. Saini, M. Singh, A.H. Reshak, M.K. Kashyap, J. Magn. Magn. Mater **331** (2013) 1.

[31] N. O. Damerdji, B Amrani, K Driss Khodja, P Aubert, J. Super.Nov. Magn **31** (2018), 2935.

[32] A. Rahmani, K. Driss Khodja, B. Amrani, Acta. Phys. Pol. A **138** (2020) 469.

[33] J. B. Goodenough, J. Phys. Chem. Solids **6** (1958) 287.

[34] R. Søndenå, P. Ravindran, S. Stølen, T. Grande, M. Hanfland, Phys. Rev. B 74 (2006) 144102.

[35] S.Vasala, M. Karppinen, Prog. Solid State. Chem. **43** (2015) 1.

[36] T.S. Chan, R.S. Liu, G.Y. Guo, S.F. Hu, J.G. Lin, J.F. Lee, L.Y. Jang, C.R. Chang, C.Y. Huang, Solid State Commun. **131** (2004) 531.

[37] H.T. Jeng, G. Y. Guo, Phys. Rev. B **67** (2003) 094438.

[38] D.P. Rai, A. Shankar, M.P. Ghimire, Sandeep, R.K. Thapa, Comput. Mater. Sci. **101**, (2015) 313.

[39] Z. Fang, K. Terakura, J. Kanamori, Phys. Rev. B **63** (2001) 180407.

[40] W. Zhong, W. Liu, C.T. Au, Y.W. Du, Nanotechnology **17**(2006)250.

[41] S.A. Ivanov, S.G. Eriksson, R. Tellgren, H. Rundlöf, M. Tseggai, Mater. Res. Bull. **40** (2005) 840.

[42] A.F. Lamrani, M. Ouchri, A. Benyoussef, M. Belaiche, M. Loulidi, J. Magn. Magn. Mater. **345** (2013) 195

[43] R. Rahmani, B. Amrani, K. Driss Khodja, A. Boukhachem, P. Aubert, J. Comp. Elec **17** (2018) 920.

[44] K. I.Kobayashi, T. Kimura, H.Sawada, K.Terakura, Y.Tokura, Nature 395 (1998) 677.

[45] Z. Szotek, W.M. Temmerman, A. Svane, L. Petit, G.M. Stocks, H. Winter, J. Magn. Magn. Mater 272(2004)**1816**.

[46] J. Zhang, W.J. Ji, J. Xu, X.Y. Geng, J. Zhou, Z.B. Gu, S.H. Yao, S.T. Zhang, Sci. Adv. **3** (2017) e1701473.

[47] T. Xia, Q. Li, J. Meng, X. Cao, Mat. Chem. Phys. **111** (2008) 335.

[48] A. Faik, M. Gateshki, J.M. Igartua, J.L. Pizarro, M. Insausti, R. Kaindl, A. Grzechnik, J. Sol. Stat. Chem. 181 (2008) 1759.

[49] U. Wittmann, G. Rauser, S. Kemmler-Sack, *Z. Anorg. Allg. Chem.* 482(1981) 143

[50] M. W Lufaso, R. B. Macquart, Y. Lee, T. Vogt, H. C. zur Loye, J. Phys.: Condens. Matter 18 (2006) 8761.

[51] A. Tauber, S.C. Tidrow, R.D. Finnegan, W.D. Wilber, Physica C 256(1996)340.

[52] P. Blaha, K. Schwarz, G. K. Madsen, D. Kvasnicka, J. Luitz, wien2k. An augmented plane wave+ local orbitals program for calculating crystal properties **2001**.

[53] K. Schwarz, P. Blaha, Solid state calculations using WIEN2k. Comp. Mat. Sci **28** (2003) 259.

[54] W. Kohn, L.J. Sham, Phys. Rev. A **140** (1965) 1133

[55] J.P. Perdew, K. Burke, M. Ernzerhof, Phys. Rev. Lett. **77** (**1996**) 3865.

[56] F. Tran, P. Blaha, Phys. Rev. Lett. 102 (2009) 226401.

[57] V.M. Goldschmidt, Naturwissenschaften **14** (1926) 477.

[58] R.D. Shannon, C.T. Prewitt, Acta Crys. B **25** (1969) 925; R.D. Shannon, Acta

Cryst. **A 32** (1976) 751.

[59] A.M. Glazer, Acta Cryst. **B28** (1972) 3384.

[60] A.M. Glazer, Phase Transit **84** (2011) 405.

[61] A. S. Sanchez, J.L. G. Munoz, J. R. Carvajal, R. S. Puche, J.L. Martinez, J. Solid. State. Chem **100** (1992) 201.

[62] S.H. Byeon, S. S. Lee, J. B. Parise, P. M. Woodward, Chem. Mater. **18** (2006) 3873.

[63] M.W. Lufaso, P.W. Barnes, P.M.Woodward, Acta Cryst. B **62** (2006) 397.

[64] F.D. Murnaghan, Proc. Natl. Acad. Sci. U.S.A. 244 (1944) 30.

[65] M. Born, K. Huang, Dynamical Theory of Crystal Lattices, Claren-don, Oxford, (1956).

[66] S.F. Pugh, Phil. Mag. **45** (1954) 823.

[67] I. N. Frantsevich, F. F. Voronov, S. A. Bakuta, Elastic Constants and Elastic Moduli of Metals and Nonmetals: A Handbook, Naukova Dumka, Kiev, Ukraine 1982.

[68] B. Rameshe , M. Rajagopalan , B. Palanivel , Comput. Condens. Matter **4** (2015) 13.

[69] N.E.H. Djezzar, K.Driss-Khodja, B. Amrani, Mater. Today Commun. **26** (2021) 102106.

[70] S. Moufok, L. Kadi, B. Amrani, K. Driss Khodja, Results in Phys **13** (2019) 102315.

[71] T. Cao, Z. Li, S.G. Louie, Phys. Rev. Lett. **114**(2015)236602.

Figures

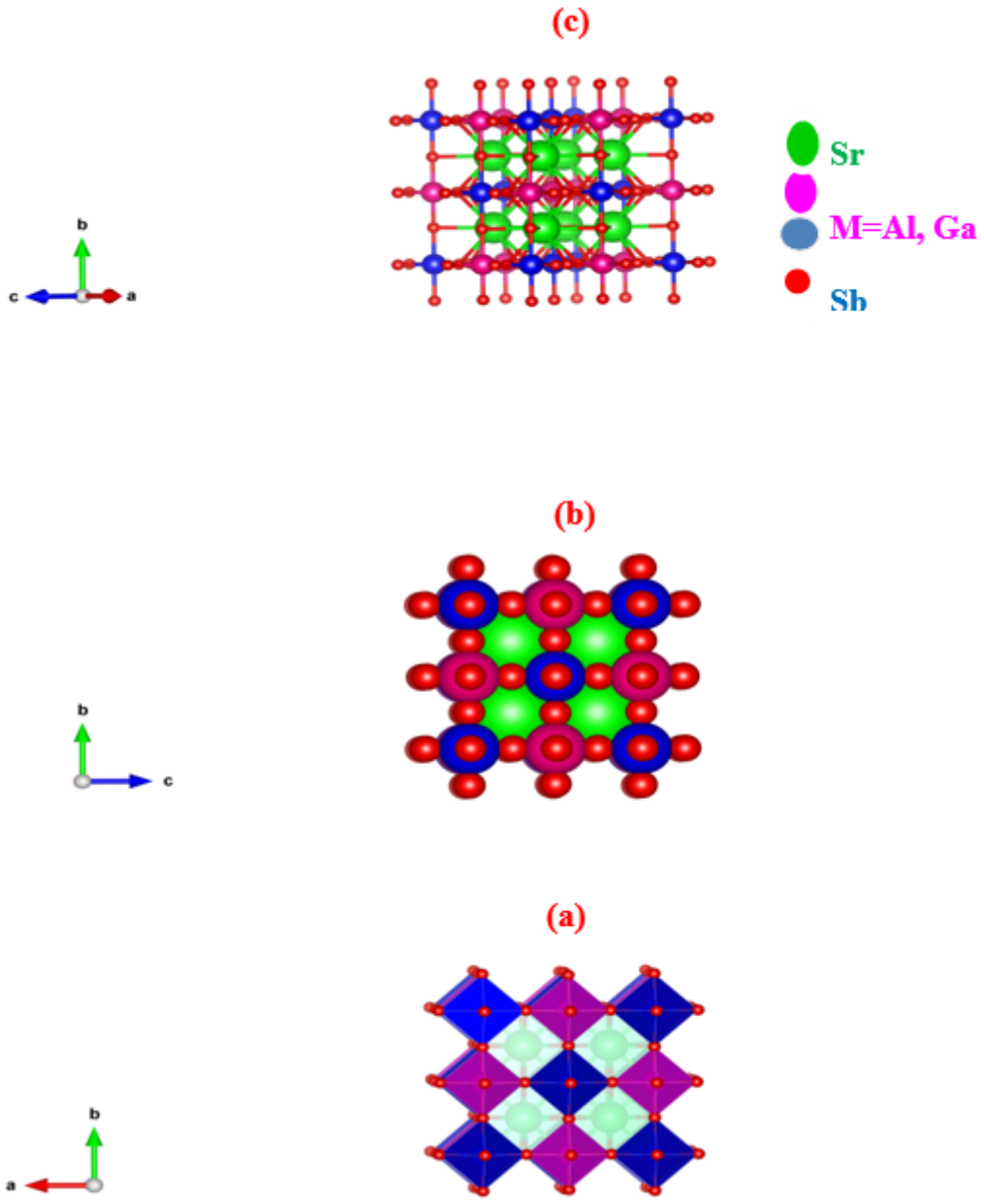

Figure 1

Structure model illustrations of cubic double perovskite oxides Sr_2MSbO_6; (**a**) polyhedral, (**b**) Space-Filling, (**c**) 3D balls and sticks

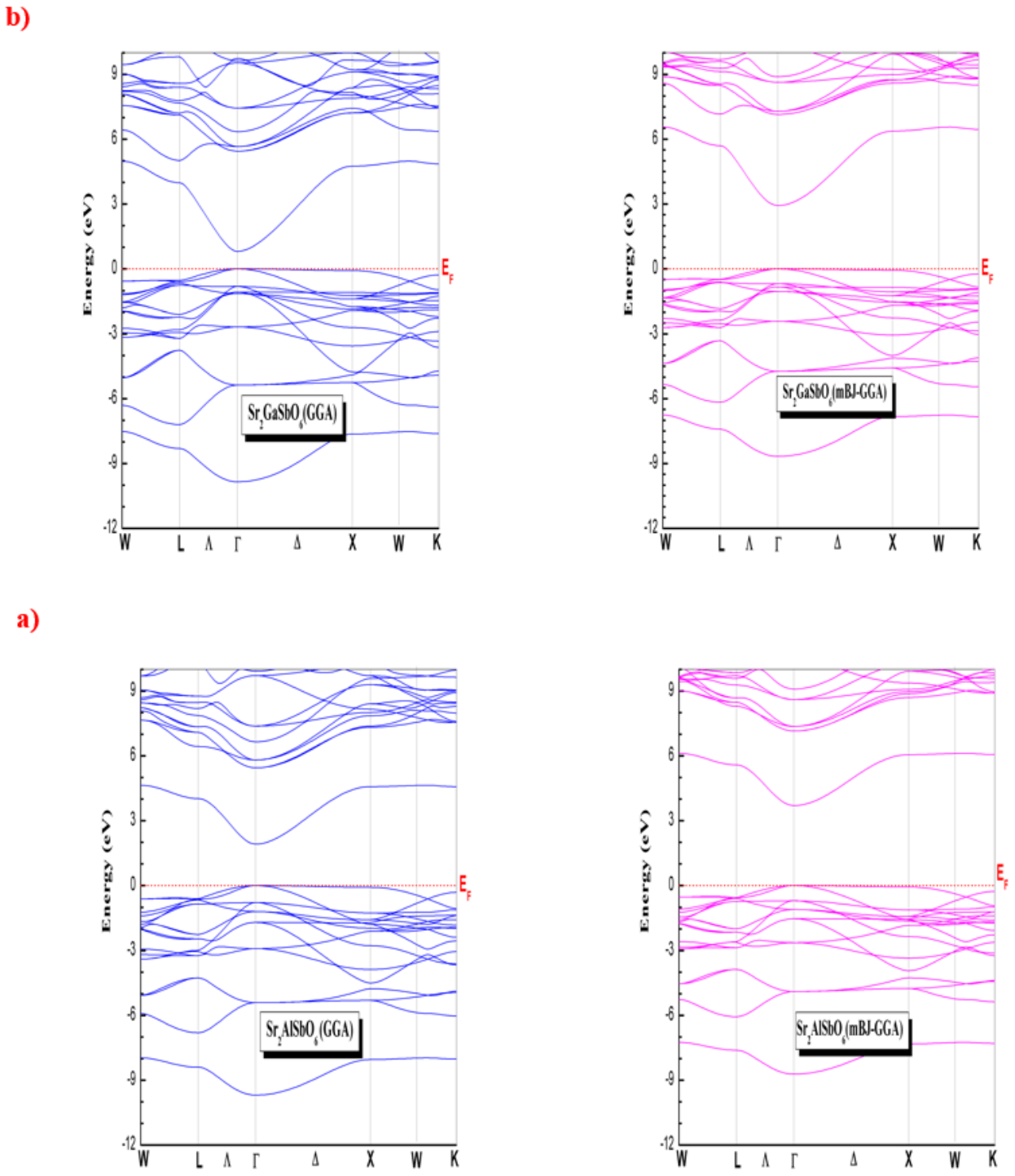

Figure 2

Band structure of the double perovskite (**a**) Sr_2AlSbO_6 and (**b**) Sr_2GaSbO_6, calculated using GGA, and mBJ-GGA.

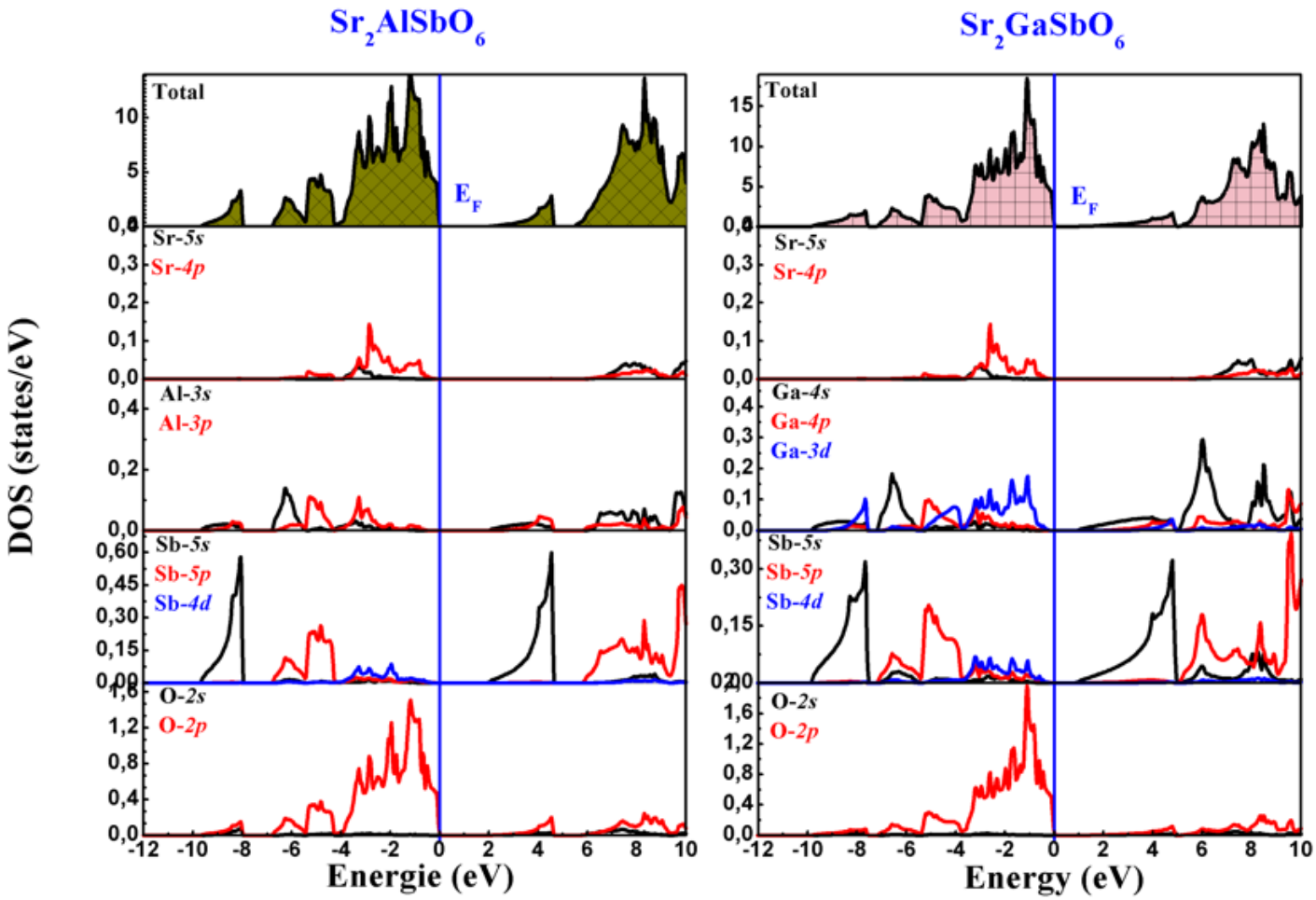

Figure 3

Density of states (DOS) plots for double perovskites Sr_2MSbO_6 (M=Al, Ga), calculated using mBJ-GGA.

Figure 4

Densities of states for doped double perovskite oxides: (**a**) $Sr_2AlSbO_{5.75}C_{0.25}$, (**b**) $Sr_2AlSbO_{5.75}N_{0.25}$, (**c**) $Sr_2GaSbO_{5.75}C_{0.25}$ and (**d**) $Sr_2GaSbO_{5.75}N_{0.25}$